Scaling and critical-like behavior in multidimensional diffusive dynamics

Savely Rabinovich and Noam Agmon
Department of Physical Chemistry and the Fritz Haber Research Center, The Hebrew University, Jerusalem 91904, Israel
(Received 11 February 1993)

The intermediate time dependence of the survival probability in two-dimensional diffusive dynamics is investigated on a model myoglobin-CO potential-energy surface. For small diffusion anisotropy, we derive a scaling relation for the characteristic time and exponent of the observed power-law dependence, which is verified by exact two-dimensional calculations. At higher anisotropy values, we report a critical-like jump in the anisotropy dependence of the power-law exponent. Possible experimental implications are discussed.

PACS number(s): 87.10.+e, 05.40.+j, 82.20.Fd, 87.15.Rn

A well-known treatment of chemical reactions in solution [1] deals with diffusive motion of the reactants over a one-dimensional (1D) potential barrier. The Kramers model has found numerous applications in chemistry and physics [2]. When chemical reactions occur in complex environments, such as inside heme proteins [3–6], more than one degree of freedom need be considered [7]. Since the stochastic motion in the system and environment coordinates will generally occur with different rates, one is led to a model of anisotropic diffusion on a multidimensional potential-energy surface. Several studies of the anisotropy dependence of the reaction rate coefficient for this problem have recently appeared [8–10]. These refer to the long-time asymptotic characteristics of the reactants' survival probability. To cope with the intermediate-time nonexponential behavior, experimentalists have developed a number of fitting formulas and *ad hoc* empirical models [3, 4]. We present a theoretical analysis of the intermediate-time regime, which we compare with exact numerical calculations. While our study is motivated by the extensive results on CO binding to myoglobin (Mb), the model presented is sufficiently simple and general to be of interest in other cases of interplay between reaction and relaxation.

We consider two-dimensional (2D) diffusion in a (dimensionless) potential field, $V(x,y)$, defined on a rectangular coordinate domain $[x_m, x_M; y_m, y_M]$. Reflective boundary conditions are imposed along the perimeter of the rectangle. V is assumed to be a double-well potential in x (but not necessarily in y). A ridgeline on the potential surface separates the domain into reactants' and products' regions, denoted by $\mathcal{R}$ and $\mathcal{P}$, respectively. For simplicity, we assume a constant, diagonal diffusion tensor, (D_x, D_y). The corresponding Smoluchowski equation describes the time evolution of the probability density, $p(x,y,t)$, for observing the system at (x,y) by time t

$$\partial_t p(x,y,t) = [D_x \mathcal{L}_x + D_y \mathcal{L}_y]\, p(x,y,t). \tag{1}$$

In Eq. (1), $\partial_t \equiv \partial/\partial t$ while $\mathcal{L}_x$ and $\mathcal{L}_y$ are Smoluchowski operators, incorporating the 2D potential

$$\mathcal{L}_z \equiv \partial_z e^{-V(x,y)} \partial_z e^{V(x,y)}, \quad z = x, y. \tag{2}$$

The initial condition, $p(x,y,0) = \delta(x - x_0)\,\delta(y - y_0)$, is chosen to be a δ function centered at some point $(x_0, y_0) \in \mathcal{R}$. It is convenient to measure time in units of D_x^{-1}, i.e., $t = \theta/D_x$. This scaling is natural when $D_x \geq 0$, since x motion is a prerequisite for barrier crossing. Equation (1) then reads

$$\partial_\theta p(x,y,\theta) = [\mathcal{L}_x + \eta \mathcal{L}_y]\, p(x,y,\theta), \tag{3}$$

where $\eta \equiv D_y/D_x$ is the "anisotropy parameter."

When $\eta \ll 1$, by the time the slow y motion begins, fast x dynamics is already governed by its lowest eigenvalue, $\kappa(y)$, which is calculated from

$$\mathcal{L}_x\, p(x,y,\theta) = -\kappa(y)\, p(x,y,\theta). \tag{4}$$

If, near some $(y, x_R) \in \mathcal{R}$, the potential is locally separable

$$V(x,y) = V_1(x) + V_2(y), \tag{5}$$

one obtains the 1D sink Smoluchowski equation [7]

$$\partial_\theta \bar{p}(y,\theta) = [\eta \mathcal{L}_2 - \kappa(y)]\, \bar{p}(y,\theta), \tag{6}$$

valid for $x \approx x_R$, where $\mathcal{L}_2 \equiv \partial_y e^{-V_2(y)} \partial_y e^{V_2(y)}$ and $\bar{p}(y,\theta) \equiv \int_{x_m}^{x_M} p(x,y,\theta)\, \chi_R(x,y) dx$. The characteristic function $\chi_R(x,y)$ equals 1 if $(x,y) \in \mathcal{R}$ and 0 otherwise. This reduction of the 2D equation to an effective 1D equation with the sink term $\kappa(y)$, analogous to the Born-Oppenheimer approximation in quantum mechanics, has been justified in several recent expositions [9, 11].

We are particularly interested in the time dependence of the survival probability

$$S(\theta) \equiv \int_{y_m}^{y_M} \bar{p}(y,\theta)\, dy = \iint_{\mathcal{R}} p(x,y,\theta)\, dx\, dy \tag{7}$$

for various anisotropy values η. By integrating Eq. (6) over y, using the reflective boundary conditions in the form $\int_{y_m}^{y_M} dy\, \mathcal{L}_2\, \bar{p}(y,\theta) = 0$, and the initial condition, $S(0) = 1$, we obtain

$$S(\theta) = \exp\left(- \int_0^\theta \langle \kappa \rangle_{\theta'}\, d\theta' \right), \tag{8}$$

 ©1993 The American Physical Society

where $\langle\kappa\rangle_\theta \equiv \int_{y_m}^{y_M} \kappa(y)\,\bar{p}(y,\theta)\,dy\,/S(\theta)$. While this result is similar to the heuristic model of Ref. [4], it follows here as the exact solution of Eq. (6). This solution is formal, since calculation of the time-dependent rate coefficient $\langle\kappa\rangle_\theta$ still requires the solution of Eq. (6). Equation (8) may serve as a basis for approximations. For example, one may assume that the normalized density $\bar{p}/S$, relaxes without widening. Relaxation will therefore be determined only by the average value of the coordinate $\langle y\rangle(t)$. For the potential considered below $V_2(y) = \frac{1}{2}\nu y^2$, so that $\langle y\rangle(t)$ will relax exponentially for large $D_y t$. Therefore

$$\bar{p}(y,\tau)/S(\tau) \approx \delta(y - \langle y\rangle) \approx \delta(y - y_0 e^{-\tau}), \tag{9}$$

where we have defined dimensionless time by $\tau \equiv \eta\nu\theta$. Inserting into Eq. (8) yields an explicit expression for the logarithmic derivative of the survival probability

$$B(\tau) \equiv -\eta\nu\,\frac{d\ln S(\tau)}{d\ln\tau} \approx \tau\,\kappa(y_0 e^{-\tau}). \tag{10}$$

We have recently shown [11] that the approximation on the right-hand side agrees semiquantitatively with the exact numerical solution of Eq. (1) in the small-η regime.

The logarithmic derivative in Eq. (10) enables the discussion of the time dependence of $S(\tau)$ for $\eta \ll 1$. As $\tau \to \infty$, $B(\tau) \to \tau\kappa(0)$ so that $S(\tau)$ decays exponentially with a rate coefficient $\kappa(0)$, where $y = 0$ represents the minimum of $V_2(y)$. This is a poor description of the anisotropy dependence of the equilibrium rate coefficient, since $\kappa(0)$ is independent of η. More insight is gained in the analysis of the intermediate-time behavior of $S(\tau)$. It will be a power law when $B(\tau) \approx$const, for example, near extrema of $B(\tau)$. Given an extremum at τ_α, one expects that $S(\tau) \propto \tau^{-\alpha}$ in the vicinity of τ_α. From Eq. (10) one finds that α is given by [11]

$$\alpha = B(\tau_\alpha)/(\nu\eta). \tag{11}$$

Since for $\eta \ll 1$, $B(\tau)$ is a universal function which is independent of both ν and η, we obtain a simple scaling relation for α in this regime. This differs, of course, from the scaling behavior of the survival probability [12]. We believe this is the first time a scaling behavior of α itself is revealed. By definition the time θ_α around which power-law behavior is observed exhibits similar scaling, $\theta_\alpha = \tau_\alpha/(\nu\eta)$. Hence the above relations may be written as

$$\alpha/\theta_\alpha = B(\tau_\alpha)/\tau_\alpha \approx \kappa(y_0 e^{-\tau_\alpha}). \tag{12}$$

In experimental systems, η will usually vary with external parameters such as temperature or solvent viscosity. Unfortunately, this dependence is not easily measured. In contrast, one may obtain both α and θ_α from a single measurement of $S(t)$.

Figure 1 shows the 2D potential-energy surface used in our study. It comes from a model [7] for CO binding to the iron-porphyrin complex in Mb. x is the Fe-CO distance, hence the well on the left represents bound CO while that on the right represents dissociated CO, trapped inside the "heme pocket." y is a "protein coordinate" depicting large-scale nonequilibrium protein motions and influencing heme reactivity *possibly* by modulation of the iron out-of-(the porphyrin plane) distance.

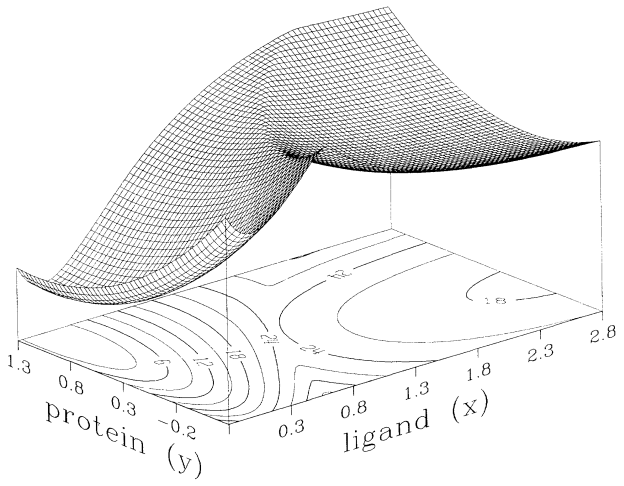

FIG. 1. The potential-energy surface for CO binding to Mb. The potential is defined by Eq. (4) in Ref. [7], with its parameters collected in Table I of Ref. [7]. The contours are labeled in kcal/mol. The dimensionless potential $V(x,y)$ is gotten by dividing the potential by k_BT, where k_B is Boltzmann's constant and $T = 200$ K ($\approx$ the solvent glass transition), so that $k_BT = 0.39$ kcal/mol. The (dimensionless) force constant for the protein coordinate is $\nu = 35.9$. The 3D plot shown above the contour plot uses the same 75×50 grid as in the numerical calculation.

Experiment [5] and molecular-dynamic simulations [13] show that both ligand and protein motions are diffusive for times longer than a few hundred picoseconds. On these time scales, the iron motion is already expected to be tightly coupled to the protein. Treatment of the ballistic iron motion at shorter times may require the introduction of an additional coordinate [14]. The reactants region $\mathcal{R}$, representing unbound Mb+CO, is on the right of the ridgeline. Though other dividing lines may be suggested, the ridgeline is a simple, reasonable choice. At the initiation of the experiment, the reactants are prepared by photodissociating MbCO which is equilibrated in $\mathcal{P}$, to the left of the ridgeline, producing an initial distribution in $\mathcal{R}$. We consider an infinitely narrow initial distribution which is placed at $(x_0, y_0) = (2.5, 1.1)$. However, we find that $\alpha(\eta)$ depends only slightly on the initial location in this region of $\mathcal{R}$. The Mb potential is cut at $y_M = 1.3$ to disallow barrier crossing in the y direction directly from the reactants' well, as this produces a finite limiting value for α [11], thus obscuring the scaling behavior for $\eta \to \infty$.

The exact solution of the Smoluchowski equation (1) has been propagated numerically as in our previous work [10] and integrated to obtain the survival probability, Eq. (7). Unlike stochastic trajectory methods, zero statistical noise is involved in the propagation of the partial differential equation. The anisotropy was varied by arbitrarily setting $D_x = 1$ and changing D_y. The survival probability was then plotted on a log-log scale and inspected visually for an inflection point θ_α. Linear regression was used to determine α, with data points eliminated from both sides of θ_α until a correlation co-

TABLE I. Parameters for the two power-law phases as obtained from diffusive dynamics on the potential-energy surface of Fig. 1. The notation is $x[y] \equiv x \times 10^{y}$.

η	α_1	θ_{α_1}	α_2	θ_{α_2}
1[-4]	5.82[-1]	2.0[1]		
1[-3]	8.49[-2]	3.0[0]	7.27[-5]	1.2[2]
1[-2]	8.89[-3]	3.4[-1]	7.33[-6]	1.2[1]
1[-1]	1.89[-4]	8.2[-2]	7.63[-7]	1.2 [0]
2[-1]	1.93[-5]	6.0[-2]	3.90[-7]	5.9[-1]
3[-1]	3.29[-6]	5.3[-2]		
4[-1]	7.52[-7]	5.6[-2]	1.96[-7]	2.7[-1]
5[-1]	2.22[-7]	6.3[-2]	1.43[-7]	1.8[-1]
1[0]	2.09[-9]	1.1[-2]	2.32[-10]	2.1[-2]
2[0]	1.88[-11]	6.4[-3]		
3[0]	8.40[-13]	4.9[-3]		
4[0]	6.81[-14]	3.8[-3]		
5[0]	9.10[-15]	3.3[-3]		
1[1]	9.89[-18]	2.0[-3]		
2[1]	5.01[-21]	1.1[-3]		
3[1]	4.65[-23]	8.3[-4]		
4[1]	1.50[-24]	6.5[-4]		
5[1]	1.01[-25]	5.4[-4]		
1[2]	1.94[-29]	3.1[-4]		

efficient better than 0.995 was obtained. This procedure is demonstrated elsewhere [11]. Using it, two distinct power-law regimes were found for $\eta \ll 1$; see Table I. The dependence of α_1 and α_2 on anisotropy is shown in Fig. 2.

To analyze this dependence in the $\eta \ll 1$ regime, we plot in Fig. 3 the universal function $\tau\kappa(y_0 e^{-\tau})$, approximating the logarithmic derivative in Eq. (10). Initially, this function increases linearly with a slope $\kappa(y_0)$. Subsequently, $y_0 e^{-\tau}$ decreases and so does κ. This follows from the shape of the potential in Fig. 1, which leads to a monotonic dependence of $\kappa(y)$ on y. Therefore $B(\tau)$ exhibits a maximum, see Fig. 3, giving rise to α_1. At large

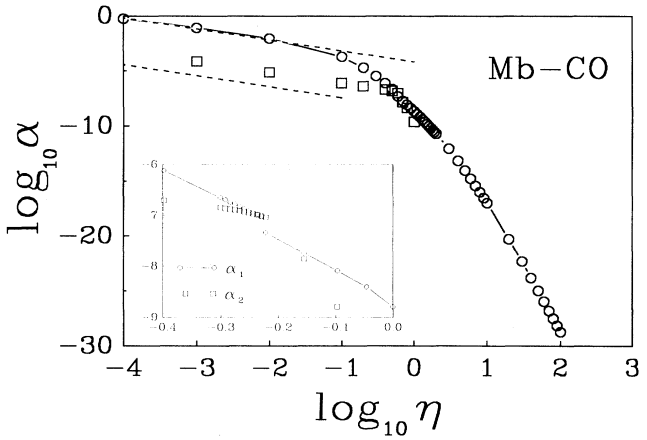

FIG. 2. Dependence of the exponents of the two power-law phases on anisotropy. α_1 is represented by open circles, connected by a bold curve to guide the eye, while α_2 is represented by open squares. The dashed curves are the approximate scaling relation, Eq. (11), using $B(\tau_{\alpha_i})$ from Fig. 3. The inset shows an enlargement of the transition region near $\eta = 1$.

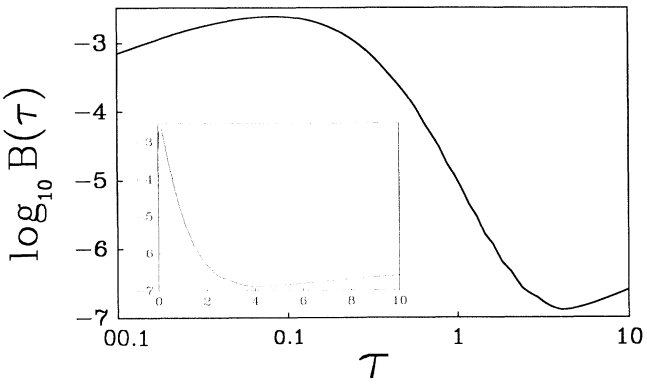

FIG. 3. The universal logarithmic derivative, as obtained from the approximation in Eq. (10). From its maximum and minimum we obtain $(\tau_{\alpha_i}, B(\tau_{\alpha_i})) = (8.41\times10^{-2}, 2.36\times10^{-3})$ and $(4.01, 1.28 \times 10^{-7})$ for $i = 1$ and 2, respectively. The inset shows the same data on a linear τ scale, emphasizing the long-time linear dependence on τ.

τ, $B(\tau)$ increases linearly with τ, $B(\tau) \approx \kappa(0)\tau$. Consequently one has a minimum in Fig. 3, which defines α_2. Thus for MbCO *two* power-law phases are predicted. The first, around the maximum in $B(\tau)$, represents the onset of protein (y motion) relaxation, while the second, near the minimum in $B(\tau)$, signals its termination.

Extracting $B(\tau_{\alpha_i})$ from Fig. 3 yields the two dashed lines in Fig. 2 representing the scaling relation (11) for α_i, $i = 1, 2$. Agreement is particularly good for α_1, indicating that the theoretical scaling law (11) describes the exact η dependence *without* any adjustable parameters. For α_2, the approximate estimate of $B(\tau_{\alpha_2})$ is inaccurate, but scaling with $1/\eta$ still holds. One also notes (Table I) that the predicted constancy of α/θ_α, Eq. (12), indeed holds for $\eta \leq 0.01$.

Theory for the $\alpha(\eta)$ dependence for larger-η values is still lacking, hence we investigate it numerically. As η approaches unity (isotropic diffusion limit) the scaling relation breaks down, and the α_i decrease much faster than $1/\eta$. The inset to Fig. 2 shows the behavior in this region. A jump in the values of α_i is observed, resembling a first-order phase transition, which is quite unexpected for a diffusive process. In this region $B(\tau)$ is no longer a universal function. Figure 4 shows its behavior as obtained from our 2D propagations. As η increases, the peak that prevailed at small η disappears and a new peak grows at a smaller value of τ. The critical value of η for this transition is around $\eta_c = 0.59$. Subsequently, there is a second kind of transition, where the new minimum in $B(\tau)$ diminishes and eventually grows negative. The value of η at which $B(\tau_{\alpha_2}) = 0$ is around 1.07. Finally, for $\eta \to \infty$ we find (Fig. 2) that $\alpha_1 \propto \eta^{-12.5}$. It is remarkable that the same trend in α_1 seems to hold over 20 orders of magnitude in the large-η region. To obtain this data, quadruple precision (32-digit accuracy) has been used on a Convex computer. As η increases, a qualitatively similar behavior is observed in less significant digits. While this self-similarity may be interesting theoretically, it is hard to see its experimental significance.

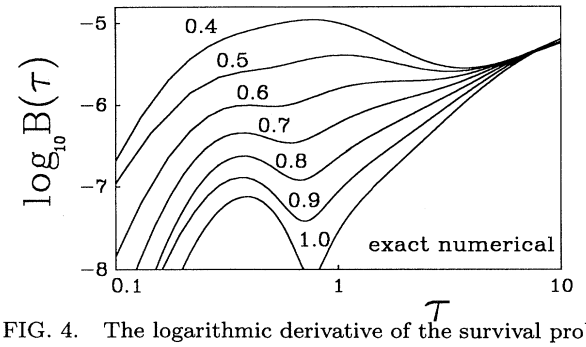

FIG. 4. The logarithmic derivative of the survival probability, as obtained from exact 2D propagations for the indicated values of η.

The physical significance of the behavior in the $\eta < 1$ regime does seem clear. An initially narrow distribution of protein conformations (y values) widens to produce a power-law decay. However, even the relaxation of a zero-width distribution, Eq. (9), will produce a power-law phase. Therefore, power-law kinetics is not limited to the case thus far monitored experimentally [4], namely, an initially wide conformational distribution. If a very narrow distribution of substates could be prepared, it should show exponential kinetics at very low temperatures and power-law kinetics developing at higher temperatures. This is just the reverse of the usual trend.

The temperature dependence of the power-law phase may be understood if one assumes that η increases monotonically with T due to increasing protein relaxation. (This neglects the weaker T dependence in the Smoluchowski operator.) As η increases, one expects the power-law regime to occur earlier and exhibit a smaller power, Eq. (11). Since α depends only weakly on initial conditions for $\eta \ll 1$, a similar behavior should occur also for a wide initial distribution [4]. Because $\theta_\alpha = D_x t_\alpha$, Eq. (12) could be used to extract the temperature dependence of D_x from kinetic data [4] just above the glass transition. At higher temperatures our calculations suggest the existence of a "critical temperature" T_c, corresponding to η_c at which α drops discontinuously to a small, unmeasurable value (Figs. 2 and 4). It would be interesting if evidence for such behavior could be found in heme protein dynamics.

The power law persists until the distribution relaxes in $\mathcal{R}$. Thereafter, binding proceeds exponentially but at a much slower rate than either initially or at low temperatures [7]. The increase of the geminate recombination barrier with temperature has been recently verified by experiment [4, 6]. This "anti-Arrhenius" slowing down of binding with increasing temperature could provide a "self-cooperativity" mechanism [7] for disabling the reverse rebinding process following ligand dissociation, thus assuring that ligand release proceeds to completion.

This work was supported by Grant No. 86-00197 from the U.S.–Israel Binational Science Foundation (BSF), Jerusalem, Israel. The Fritz Haber Research Center is supported by the Minerva Gesellschaft für die Forschung, München, FRG.

[1] H. A. Kramers, Physica **7**, 284 (1940).
[2] Ber. Bunsenges. Phys. Chem. **95**, No. 3 (1991).
[3] R. H. Austin, K. W. Beeson, L. Eisenstein, H. Frauenfelder, and I. C. Gunsalus, Biochem. **14**, 5355 (1975).
[4] P. J. Steinbach *et al.*, Biochem. **30**, 3988 (1991); R. D. Young *et al.*, Chem. Phys. **158**, 315 (1991).
[5] M. K. Hong, E. Shyamsunder, R. H. Austin, B. S. Gerstman, and S. S. Chan, Phys. Rev. Lett. **66**, 2673 (1991).
[6] W. D. Tian, J. T. Sage, V. Šrajer, and P. M. Champion, Phys. Rev. Lett. **68**, 408 (1992).
[7] N. Agmon and J. J. Hopfield, J. Chem. Phys. **78**, 6947 (1983); **79**, 2042 (1983); **80**, 592(E) (1984).
[8] M. M. Kłosek-Dygas, B. M. Hoffman, B. J. Matkowski, A. Nitzan, M. A. Ratner, and Z. Schuss, J. Chem. Phys. **90**, 1141 (1989); B. Carmeli, V. Mujica, and A. Nitzan, Ber. Bunsenges. Phys. Chem. **95**, 319 (1991).
[9] A. M. Berezhkovskii and V. Yu. Zitserman, Physica A **166**, 585 (1990); Chem. Phys. **157**, 141 (1991); **164**, 132 (1992).
[10] N. Agmon and R. Kosloff, J. Phys. Chem. **91**, 1988 (1987); N. Agmon and S. Rabinovich, Ber. Bunsenges. Phys. Chem. **95**, 278 (1991); S. Rabinovich and N. Agmon, Chem. Phys. Lett. **182**, 336 (1991).
[11] N. Agmon and S. Rabinovich, J. Chem. Phys. **97**, 7270 (1992).
[12] T. G. Dewey and J. G. Bann, Biophys. J. **63**, 594 (1992).
[13] G. Verkhivker, R. Elber, and Q. H. Gibson, J. Am. Chem. Soc. **114**, 7866 (1992); Q. H. Gibson, R. Regan, R. Elber, J. S. Olson, and T. E. Carver, J. Biol. Chem. **267**, 22 022 (1992).
[14] V. Šrajer, L. Reinisch, and P. M. Champion, J. Am. Chem. Soc. **110**, 6656 (1988).